Steady and Oscillatory Shear Flow Alignment Dynamics in a Lamellar Diblock Copolymer Solution

Janice L. Zryd[†] and Wesley R. Burghardt*

Department of Chemical Engineering Northwestern University Evanston, Illinois 60208

Received July 21, 1997; Revised Manuscript Received March 9, 1998

ABSTRACT: Shear flow alignment in a symmetric polystyrene−polyisoprene (PS−PI) diblock copolymer solution in dioctyl phthalate has been studied using flow birefringence and rheology. In large amplitude oscillatory shear, we find behavior similar to that previously reported in lamellar PS−PI melts. At high reduced frequency, parallel alignment of the layers is preferred, confirmed with birefringence measurements using oblique light paths. At low reduced frequency, perpendicular alignment is favored. In steady shear flow experiments well below the ODT, a similar behavior pattern is found: perpendicular alignment results at low shear rates, and parallel alignment is found at high shear rates. These are the first results demonstrating flipping by a change in *steady* shear flow conditions. As temperature is increased, the degree of perpendicular alignment obtained at low reduced shear rates decreases, unlike the behavior in large amplitude oscillatory flow, where high degrees of perpendicular alignment are achieved at low frequencies even close to the ODT. This suggests that flow alignment in steady shear is more complex than that in oscillatory shear flow, perhaps owing to an increased likelihood for defect formation. Finally, no flow-induced changes were observed in the order−disorder transition in either steady or large amplitude oscillatory shear flow.

1. Introduction

Block copolymers have been the object of intensive scientific interest during recent decades. Unique and useful properties result from mating dissimilar chain types. In many cases, these properties are derived from microphase separation, driven by thermodynamic incompatibility between the blocks, constrained by chain connectivity to macromolecular length scales. Even the simplest example, a diblock copolymer with varying degrees of polymerization (N), interaction parameters (χ) and fractional compositions (f), has provided impetus for volumes of experimental and theoretical research aimed at understanding how these (and perhaps other, more subtle) variables interact in determining the conditions at which microphase separation occurs, and the resulting ordered morphology. Review articles by Bates and Fredrickson provide an overview of this fascinating subject.[1] Block copolymers offer an irresistible opportunity for polymer chemists and physicists, as diverse microscopic structures may be generated, and controlled, through careful design and synthesis of ever increasingly complex multiblock copolymer architectures.

Among their many facets, block copolymers exhibit complex dynamics when subjected to external mechanical fields. Of particular interest has been the phenomenon of *flow alignment*, whereby macroscopic orientation is induced in ordered block copolymers with an initially random distribution of grain orientations. Keller and co-workers were the first to report this behavior over 20 years ago,[2,3] motivating study by many groups.[4−10] However, a flurry of recent research on flow alignment of well-characterized diblocks has been motivated by the discovery that shear flow is capable of inducing *different* orientation states in the same material, depending on alignment conditions (temperature, oscillatory shear flow frequency, and strain, etc.).[11−13] This suggests the rich physics possible when weakly ordered materials are subjected to mechanical deformation, demonstrated by a sometimes frustrating diversity of phenomena observed in the many studies that have studied flow alignment in model diblocks in detail.[11−29] Given the infinite range of complexity in molecular architecture and phase behavior possible in block copolymers, it is telling that these recent studies of nonlinear flow behavior have focused primarily on symmetric diblocks: even in this, the simplest case, it has proven challenging to obtain a consensus about the nature of flow alignment phenomena and their underlying mechanisms.

The most exhaustive studies of flow alignment dynamics have been performed on symmetric styrene−isoprene (PS−PI) diblock copolymers, either in the melt[12−16,18−20,25−29] or solution.[21−23] Both ex situ (SAXS[12−15,19,24−29] and TEM[12,13,16]) and in situ (birefringence[17−20] and neutron scattering[21−23]) structural probes have been used to characterize morphological changes that occur during flow alignment, mostly using large amplitude oscillatory flow. The various techniques offer different advantages. Other things being equal, in situ experiments are preferable. Of these methods, birefringence offers superior time resolution to neutron scattering but provides a less comprehensive representation of the orientation state than scattering methods. Off-line SAXS studies on shear-aligned samples provide the opportunity to systematically probe all possible lamellar orientations in the sample, although studies have typically focused only on populations in the three principal coordinate planes defined by the shear geometry. None of the bulk techniques (birefringence or scattering) can provide information about defect structure or local grain organization in the textured block copolymer. In general,

* To whom correspondence should be addressed: w-burghardt@nwu.edu.

[†] Present address: The Dow Chemical Company, Midland, MI 48674.

S0024-9297(97)01091-7 CCC: $15.00
Published on Web 05/13/1998

understanding is most advanced where different groups have obtained self-consistent results on different samples using different methods.

In symmetric PS−PI diblock melts, it is generally reported that parallel alignment results at high frequencies, where comparatively local chain motions are probed. In this regime, it is hypothesized that viscoelastic contrast between the rigid styrene (near T_g) and rubbery isoprene (far above T_g) blocks favors parallel alignment (layer normals parallel to the velocity gradient). Even within this regime, there is a complex transition in the alignment trajectory, dependent upon both frequency and strain amplitude, whereby preferential depletion of transverse (layer normals parallel to the flow direction) or perpendicular (layer normals parallel to the vorticity direction) populations is the initial step on the path toward ultimately parallel orientation.[18,19] These intermediate states appear to be connected to reports of biaxial orientation,[15,24,26] where the relative populations along the three shear axes evolve differently during the alignment depending on the particular conditions.

As frequency is reduced, alignment dynamics change and perpendicular alignment is favored.[12−14] Near the critical frequency, it is also possible to flip between perpendicular and parallel alignment by changes in the applied *strain*.[20] To a first approximation, this transition frequency is shifted in a straightforward way with temperature, due to shifts in the polymer relaxation dynamics.[14,19] At still lower frequencies, Zhang and coworkers have reported the existence of an additional parallel alignment regime;[25,27,28] however, others have not found such a regime in PS−PI melts.[14,19] It appears that this discrepancy follows from differences in thermal history during sample preparation, adding yet another variable that impacts flow alignment dynamics.[27] In the perpendicular alignment regime, it has also been reported that alignment reverts to parallel below some fairly low critical strain.[29]

While much work has focused on PS−PI melts, Balsara and co-workers have also studied concentrated solutions of PS−PI block copolymers in a neutral solvent.[21−23] While they observe some phenomena similar to melts (the ability of oscillatory shear flow to generate high parallel orientation, for instance[21,22]), there are some differences. For instance, Wang et al. only observe high degrees of perpendicular alignment in a transient state, and at high oscillation frequencies and amplitudes they cite evidence for shear-induced disordering.[23] Compared to the above studies on melts, however, Balsara and co-workers have not covered a wide range of parameter space, and direct comparison is hampered by the lack of rheological data which could be used to define characteristic material relaxation times.[21−23]

In this paper we report results of extensive studies of flow alignment dynamics in a symmetric PS−PI diblock copolymer solution. One objective is to identify the extent to which concentrated solutions mimic the behavior of PS−PI melts, taking advantage of rheological characterization in addition to in situ birefringence studies of orientation development. In addition to large amplitude oscillatory flow, we also are studying alignment dynamics in steady shear flow. Given that strain amplitude has been proven to be an important variable in oscillatory flow alignment dynamics, it is reasonable to expect some differences in behavior in steady flow, where arbitrarily large strains accumulate during the course of alignment. Comparatively little attention has been paid to steady shear flow alignment in these recent studies,[12,21,22] and it is not known, for instance, whether flipping between orientation states may be accomplished in steady shear flow by variations in shear rate or temperature. Our second principal objective, then, is to fill this gap to some extent and to motivate further work in this direction. Finally, it is appreciated that previous birefringence measurements using a single projection are potentially ambiguous concerning the degree of parallel alignment in lamellar systems,[18] although supplementary scattering measurements allow interpretation of birefringence data with greater confidence.[19] Here we illustrate an approach whereby complementary measurements using oblique light paths can also supplement traditional birefringence data to confirm assignment of parallel alignment states.

2. Experimental Section

2.1. Sample. The polystyrene−polyisoprene diblock copolymer was synthesized by anionic polymerization, using procedures described elsewhere.[30] The composition was determine by UV absorption measurements to be 53% PS by mass, leading to a volume fraction $f_{PS} = 0.50$ using tabulated specific gravity data for PS and PI. Gel permeation chromatography (GPC) showed that the polydispersity was = 1.08. Molecular weights were determined by GPC in tetrohydrofuran using interpolation between calibration curves for polyisoprene and polystyrene homopolymer with the procedures of Runyon *et al.*[47,48] This led to a value $M_w = 77\,800$. An independent measure of molecular weight was obtained from intrinsic viscosity measurements. At 35 °C, the intrinsic viscosity of the block copolymer in toluene is 0.56 dL/g. Mark−Houwink constants obtained from literature intrinsic viscosity data on symmetric, anionically synthesized PS−PI block copolymers[31,32] yield a molecular weight $M = 81\,000$. On the basis of these two values, we report of sample molecular weight of 79 000 ± 3000.

As a result of its symmetric composition, microphase separation is expected to occur in a lamellar morphology in the melt. It is generally accepted that dioctyl phthalate (DOP) acts as a nonselective solvent for PS−PI block copolymers,[22,33] although it is expected that the local solvent concentration will be enhanced in the interfacial regions.[34,35]

Our solution was prepared at a concentration of 34 wt % PS−PI in DOP by first dissolving the polymer into chloroform while stirring. After adding an appropriate amount of dioctyl phthalate, the solution was stirred for several more hours. Chloroform was removed by placing the solution in a vacuum oven and evaporating until the solution reached the constant weight expected for the polymer and DOP. Evaporation of chloroform was accompanied by a negligible loss of DOP due to its low volatility. The volume fraction of block copolymer, ϕ, equals 0.34, as well.

Previous research suggests that viscoelastic contrast plays a significant role in determining flow alignment in PS−PI melts, due to proximity to the glass transition of the polystyrene block at temperatures where alignment experiments have been performed[14,18,25] (although viscoelastic contrast may also involve more subtle molecular variables[1]). Using differential scanning calorimetry (Perkin-Elmer DSC 7), the glass transition temperature of our solution was measured to be −80 °C, significantly outside of the range in which alignment experiments are performed in this study.

2.2. Mechanical Rheometry. A Bohlin VOR rheometer was used for mechanical experiments. A narrow gap Couette fixture was employed in all experiments to facilitate measurements over a range of temperature. In oscillatory shear flow, strain sweeps revealed linear viscoelastic behavior for strains below 1%; all dynamic measurements were consequently performed at strains ranging from 0.3 to 1% so that the

oscillatory testing would not induce changes in the orientation state of the lamellar domains.

Flow alignment experiments in steady shear flow were performed in the rheometer using either continuous or intermittent shear flow; shear stress was monitored during the steady shearing. In intermittent experiments, shear was periodically stopped, and linear frequency sweeps performed to monitor evolution of the viscoelastic properties of the block copolymer solution. A limited number of alignment experiments were performed using large amplitude oscillatory flow in the Bohlin rheometer. In oscillatory mode, however, the rheometer provides a maximum strain of only 20%. While sufficient to induce significant changes in the orientation and rheological properties, experiments at this modest strain do not appear to reach steady state even after prolonged shearing. A summary of these results may be found elsewhere.[36]

2.3. Optical Rheometry. 2.3.1. Relationship between Birefringence and Alignment in Ordered Block Copolymers. A quiescent "single crystal" ordered block copolymer with lamellar morphology will exhibit uniaxial optical anisotropy oriented along the normal to the lamella, with a value of Δn_o. In a lamellar BCP, Δn_o has two origins: (1) intrinsic birefringence associated with chain stretching along the normal direction, and (2) form birefringence associated with the periodic variation in bulk refractive index in the microphase separated layers. In materials with large contrast in refractive index (such as PS−PI), form contributions may be expected to account for the majority of birefringence.[37] These may be estimated using a standard formula for form birefringence in layered media; the result is negative (i.e., the refractive index for light polarized along the normal is less than for light polarized parallel to the lamellae).[38] In our PS−PI solution, assuming that the layers are perfectly segregated and that solvent is uniformly distributed, such an estimate leads to a form birefringence of -2×10^{-4}.[36]

When block copolymers are quenched into the ordered state, they assume a textured, "polydomain" state in which locally uniaxial grains are randomly oriented, such that there is no macroscopic alignment or optical axis. Although a small amount of light may pass through crossed polarizers due to depolarization, such a sample exhibits near zero bulk birefringence, despite the high *local* degree of anisotropy. Use of birefringence to study development of flow alignment rests on the assumption that, once a bias is introduced in the orientation state, a measurement of bulk birefringence will reflect the average degree of alignment in a textured sample. A similar assumption has been tested and productively employed using birefringence to measure bulk orientation in liquid crystalline polymers.[39]

Although form birefringence is estimated to be large, a bias in chain orientation normal to the layers is induced by the microphase separation, leading to an intrinsic contribution to Δn_o.[37] In the quiescent state, both sources of birefringence lead to uniaxial optical anisotropy, and bulk birefringence may be used to follow lamellar orientation state regardless of its microscopic source (intrinsic vs form). *During* shear, flow might distort chain conformations away from the lamellar normal, and the intrinsic contribution to the birefringence need not track the lamellar orientation state: interpretation of birefringence is potentially complex. However, we believe that under the conditions of the experiments reported here, birefringence is dominated by lamellar orientation with only weak influence of flow-induced changes in the intrinsic portion of the birefringence. Much of our reported data were obtained in a quiescent state where these concerns disappear. Further, under most conditions, we found no difference in birefringence measured during flow and following flow cessation, indicating that any flow-induced chain stretching had a negligible influence on the measured birefringence (exceptions to this are considered in Figure 11 below). Possible effects of flow-induced changes in intrinsic birefringence will be discussed further at various points in the paper.

2.3.2. Optical Train. Flow birefringence was measured using a crossed polarizer optical train, in which light intensity is measured between crossed (⊥) polarizers oriented at ±45° with respect to the flow direction (in the flow cells used here, the optical axis of the sample is parallel to the flow). Complementary measurements of intensity between parallel (||) polarizers allow normalization of the measured light intensity, so that birefringence may be calculated using

$$N^{\perp} = \frac{I^{\perp}}{I^{\perp} + I^{\parallel}} = \sin^2\left(\frac{\pi \Delta n d}{\lambda}\right) \tag{1}$$

where Δn is the birefringence, d is the optical path length, and λ is the wavelength. In these experiments, a HeNe laser was used as the light source, so that $\lambda = 633$ nm.

2.3.3. Flow Cells. Several flow cells were used for flow birefringence measurements during flow alignment of our PS−PI block polymer solution. The primary flow cell was a rotating parallel disk device constructed using optical windows. This flow cell was equipped for temperature control, using two Minco Kapton heaters placed on the outer side of each disk and a water jacket cut into the aluminum block from which the flow cell was machined. Each heater was sealed between a thin aluminum disk which faced the window and a machinable ceramic disk on the opposite side. A temperature sensor placed between the heating element and the lower (fixed) optical window was used as an input to a temperature controller. The temperature control was calibrated by inserting a thermocouple directly into the sample between the two glass plates. Holes were drilled through the heating elements to allow the laser beam to pass through the sample parallel to the rotation axis but displaced sufficiently far away from the center such that the flow field was effectively homogeneous. Optical anisotropy was thus probed in the flow-vorticity plane. The flow cell was driven using a Compumotor microstepping motor under the control of a Model 4000 Indexer. A circular contour option on the indexer provides the ability to perform oscillatory shear deformation using sinusoidal strain input. Further details of the flow cell construction are provided elsewhere.[36]

Two other flow cells were used for supplementary flow birefringence measurements at room temperature. Both allow use of oblique light paths through the shear flow, enabling measurement of the three-dimensional refractive index tensor. Such methods have been developed in our lab and applied to studies of molecular orientation in liquid crystalline polymers[40] and to measurements of the full stress tensor in sheared flexible polymers.[41,42] Here we briefly describe how these techniques may be applied to flow aligned block copolymers.

Shear flow coordinates (1, 2, 3) are defined where "1" is the flow direction, "2" is the velocity gradient direction, and "3" is the vorticity direction. Relative to these coordinates, the refractive index tensor takes the following form:

$$\mathbf{n} = \begin{pmatrix} n_{11} & n_{12} & 0 \\ n_{12} & n_{22} & 0 \\ 0 & 0 & n_{23} \end{pmatrix} \tag{2}$$

If light is sent along the velocity gradient (2) direction, as in the temperature controlled flow cell, the measured birefringence is $\Delta n = n_{11} - n_{33}$ (we designate such measurements $\Delta n_{1,3}$). If instead, the light path makes an angle θ with respect to the 2 axis within the 1,2 plane, the birefringence will be a function of angle as well as all components of the refractive index tensor

$$\Delta n(\theta) = \Delta_1 \cos^2\theta + \Delta_2 + 2n_{12} \sin\theta \cos\theta \tag{3}$$

where $\Delta_1 = n_{11} - n_{22}$ and $\Delta_2 = n_{22} - n_{33}$. Measurements of $\Delta n(\theta)$ thus provide the opportunity to fully characterize the refractive index tensor.

In anticipation of the orientation states expected for flow aligned lamellar systems, it is useful to specialize eq 3 for the particular cases of perpendicular and parallel alignment. For either case, the 1,2-component should be zero. In addition, either case should be characterized by a uniaxial distribution

of orientation, such that a *single* value of birefringence, Δ, may be defined to characterize the degree of optical (and hence structural) anisotropy.

For parallel alignment, $n_{11} = n_{33} \neq n_{22}$, and we can set $\Delta = \Delta_2 = -\Delta_1$. Under these circumstances, eq 3 reduces to

$$\Delta n(\theta) = \Delta \sin^2 \theta \quad \text{(parallel alignment)} \tag{4}$$

Note that at normal incidence ($\theta = 0$), parallel alignment gives zero anisotropy, and hence standard birefringence measurements in the 1−3 plane are insensitive to the degree of parallel alignment that may be present.[18,19] If the alignment is perfect in this geometry, $\Delta = \Delta n_o$, defined earlier.

For perpendicular alignment, we again expect uniaxiality, but with $n_{11} = n_{22} \neq n_{33}$, and we instead define $\Delta = \Delta_2$, while $\Delta_1 = 0$. Then eq 3 becomes:

$$\Delta n(\theta) = \Delta \text{ (perpendicular alignment)} \tag{5}$$

In this case, the measured birefringence should be independent of the angle of the light path in the shear plane. For perfect perpendicular alignment, $\Delta = -\Delta n_o$ (note that since Δn_o is expected to be negative in PS−PI due to the dominance of form effects, perpendicular alignment should be characterized by a large *positive* value of birefringence).

The oblique light path methods were implemented using two different flow cells. The first is a rotating disk flow cell used by Hongladarom and Burghardt,[40] of a design similar to the cell described above but machined in such a way that light can be passed through the flow cell over a range of angles within the shear plane. It may be used in either steady or oscillatory shear flow, but due to refraction at the air-window interfaces, the maximum angle $|\theta|$ within the shear flow field is around 30°. In this flow cell, significant refraction at the air−window and window−fluid interfaces also introduces polarization effects that may be accounted for using Fresnel refraction coefficients; full equations are given in ref 40. The second flow cell is described by Brown and co-workers,[41] and provides linear shear flow between two prisms with faces cut to allow light to pass through the shear flow at $\theta = 30°$ and 60° without suffering refraction effects. However, it has a restricted strain range and can thus only be used for oscillatory shear flow measurements.

2.3.4. Complications. When working with the linear shear prism flow cell, light paths are sufficiently long at steep angles that the optical retardation passes beyond the first order in eq 1. In these cases, the correct retardation order was determined by viewing the sample through crossed polarizers in white light, and referring to a Levy color chart. Once the correct order was known, the HeNe laser was used for quantitative Δn measurements. Another limitation of the crossed polarizer technique is insensitivity to the sign of the birefringence. A zero-order quarter wave plate was periodically inserted into the optical train with its slow axis parallel or perpendicular to the flow direction to confirm the sign of the sample birefringence.

A final complication arises due to nonzero baseline values of intensity between crossed polarizers. These have many possible sources including stress birefringence in the flow cell windows, electronic background, imperfect polarizer alignment, and the possible influence of depolarization from texture.[43] Many of these sources vary with exact experimental conditions, so that systematic correction of the data is not practical. For small birefringence, $I^{\perp}$ varies quadratically with Δn. The result is that modest baseline offsets in $I^{\perp}$ can lead to appreciable values of Δn when eq 1 is used.[36] These issues are significant only when the sample birefringence is small and have the effect that true zero values of birefringence are never observed.

3. Results and Discussion

3.1. Determination of the Order−Disorder Transition. Viscoelasticity in the terminal regime typically provides a good indicator of the order−disorder transition in block copolymers, since the low frequency storage and loss moduli are strongly enhanced in the ordered phase relative to their terminal behavior.[1] Our solution has an ODT near the maximum controllable temperature of the rheometer. In the narrow temperature range available above the solution ODT, we fail to observe the expected liquidlike terminal behavior (see Figure 6 below), perhaps due to limitations on sensitivity. For this reason, alternate strategies were used to determine the ODT.

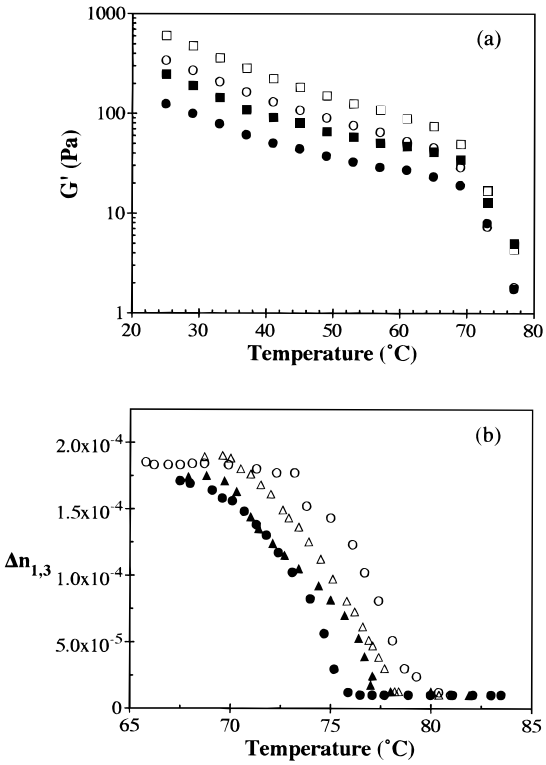

Figure 1. Determination of the ODT. (a) Storage modulus monitored at $\omega = 2.51$ (○,●) and 6.28 (□,■) rad/s and 0.3% strain as temperature is increased in 4 °C intervals. Filled symbols represent sample presheared at 91.9 s^{-1} for 300 strain units at room temperature, while open symbols represent a sample which was cooled from 85 °C without any flow. (b) Birefringence during heating (open) and cooling (closed) at 0.1 °C/min (△,▲) and 1 °C/min (○,●), while sample is subjected to oscillatory flow at 0.1 rad/s and 200% strain.

Flow alignment strongly changes the linear viscoelastic properties of an ordered BCP solution; this provides the basis for the rheological determination of the ODT presented in Figure 1a. The solution was heated above the ODT to clear thermal history, and then cooled to room temperature. In one experiment, the sample was then heated in 4° intervals, and moduli were measured at several frequencies as temperature was increased. A similar experiment was then performed in which the sample was initially sheared at room temperature, resulting in a substantial drop in dynamic moduli. The differences in moduli between the sheared and unsheared states are maintained until the ODT, where the two sets of data converge; this occurs at a temperature of 73 °C.

Figure 1b shows a rheo-optical determination of the ODT, in which a sample is subjected to low frequency, large amplitude oscillatory flow while being cooled and heated through the ODT. Appearance or disappearance of birefringence provides the indication of the ODT. At

a heating rate of 1 °C/min there is hysteresis of around 5 °C between the heating and cooling curves; however, at a lower rate this hysteresis is substantially reduced. These data suggest an ODT of 77−78 °C. Combining the two results, we conclude that the ODT for our PS−PI solution is 75 ± 3 °C.

Lodge and co-workers have recently published an extensive compilation of ODTs observed in PS−PI melts and concentrated solutions in nonselective solvents.[35] Their results demonstrated the surprising failure of the dilution approximation; instead, they found that transition temperatures and compositions for a large number of PS−PI block copolymers could be correlated by:

$$(\phi^{1.60}\chi N)_{\mathrm{ODT}} = \frac{F(f)}{2} \tag{6}$$

a form suggested by blob theory for block copolymer solutions in the semidilute limit.[34,44] $F(f)$ is a composition-dependent function from mean field theory, that assumes the value of 21 for symmetric diblocks. Using the conventions of Lodge et al.,[35] $N = 814$ for our solution, which yields $\chi = 0.0724$ at our ODT of 75 °C. This agrees with the expression for $\chi(T)$ given by Lodge and co-workers to within 1%.[35]

3.2. Effect of Shear Flow on the ODT. The ability of shear flow to change the ODT has been theoretically predicted,[45] and experimentally observed,[46] including in a PS−PI solution similar to the one studied here.[21] For this reason, we carried out a systematic study using protocols similar to those from Figure 1b to determine the effect of shear on the ODT. These experiments were conducted at 1 °C/min heating and cooling, so that the mild hysteresis observed in Figure 1b is also present in these results.

Figure 2 shows rheo-optical determination of the ODT upon heating and cooling in oscillatory shear flow for a range of frequencies. Although the magnitude of the induced birefringence varies, there is no change in the transition temperature for this range of frequencies. The heating data in Figure 2b include a sample that had been shear aligned and then heated in the quiescent state. There is no difference in the ODT measured with or without flow, to within experimental error. Oscillatory flow experiments in which strain amplitude was varied similarly showed no effect on the ODT.[36]

Figure 3 shows similar measurements obtained during steady shear flow at rates spanning 3 orders of magnitude. Note that at the lowest shear rate there is relatively little accumulation of strain on the time scale of the cooling/heating cycle, so that the birefringence assumes a relatively low value. These data, again, show no significant effect of shear flow on the ODT. These results are in disagreement with the observations of Balsara and Hammouda, who reported shear-induced increases of the ODT by as much as 20 °C, using steady shear rates up to around 40 s^{-1}.[21] They observed flow-induced anisotropy in neutron scattering patterns above the ODT, which would disappear upon cessation of shear flow. While different techniques are used here, the presence of anisotropic concentration fluctuations sufficient to generate measurable anisotropy in the scattering pattern should also generate form birefringence in the corresponding optical experiment. While our experiments cover a similar dimensional shear rate range, there are sufficient differences in sample molecular weight, concentration, proximity to T_g, etc., that there is no rational way to compare rates on a reduced basis, using a characteristic material relaxation time. Thus, it is possible that our experiments were unable to access a sufficiently high *scaled* shear rate to see the phenomena observed by Balsara and Hammouda.

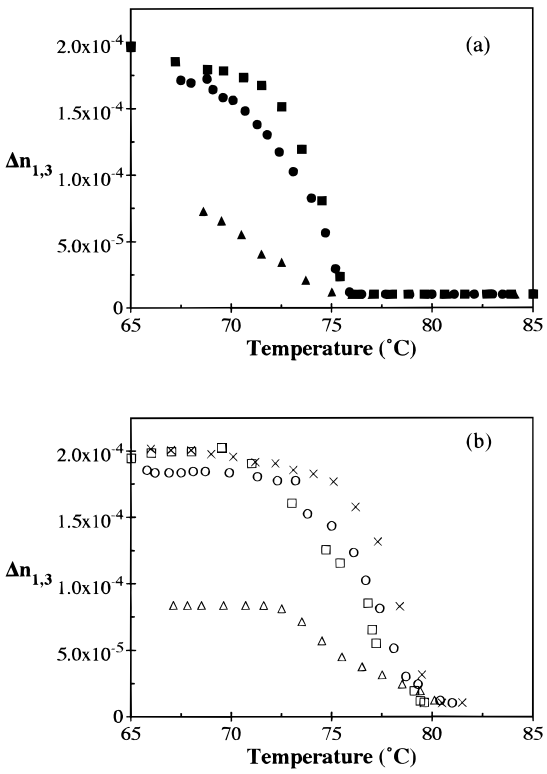

Figure 2. Effects of varying frequency during large amplitude oscillatory shear at a constant strain of 200% while (a) cooling and (b) heating at 1 °C/min: (○,●) 0.1 rad/sec; (□,■) 1 rad/sec; (△,▲) 3 rad/sec; (×) no flow (heating only).

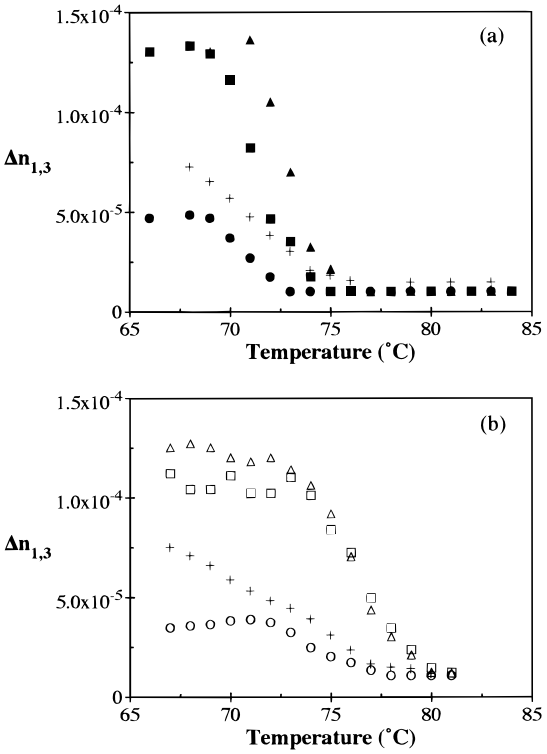

Figure 3. Effects of varying steady shear rate while (a) cooling and (b) heating at 1 °C/min: (○,●) 0.0292 s^{-1}; (□,■) 0.292 s^{-1}; (△,▲) 2.92 s^{-1}; (+) 29.2 s^{-1}.

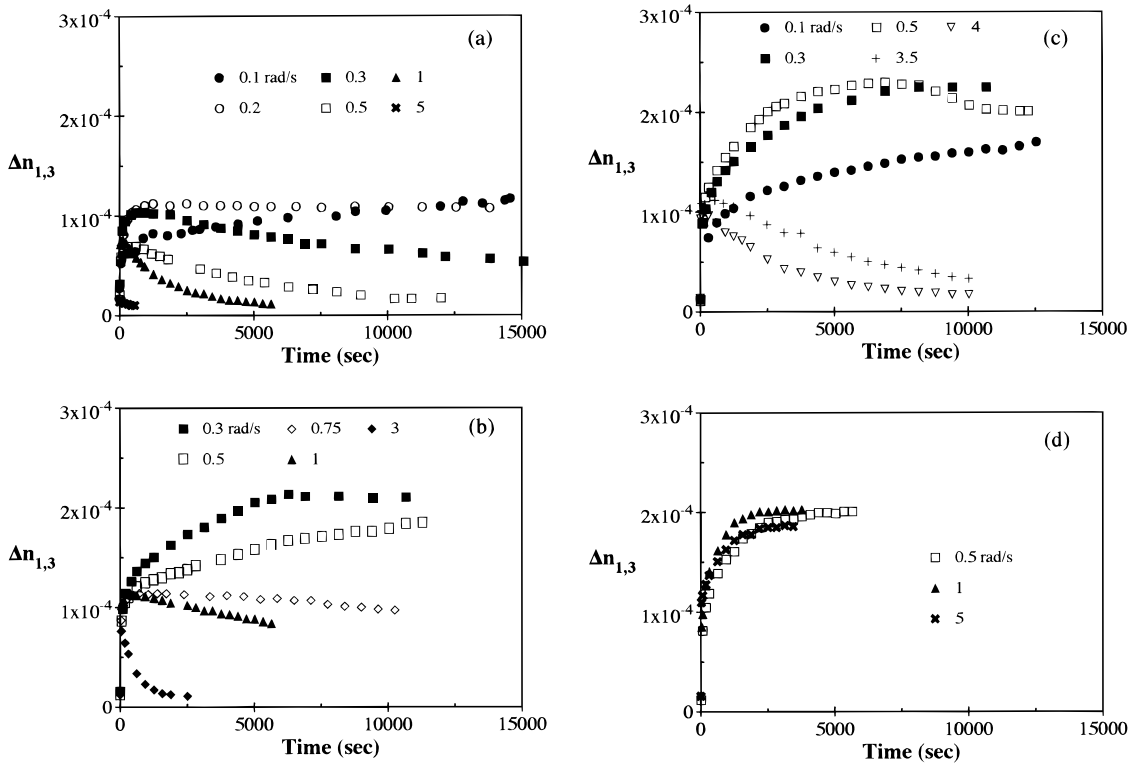

Figure 4. Birefringence during large amplitude oscillatory shear at a constant strain of 200%, and indicated frequency: (a) 25 °C; (b) 35 °C; (c) 50 °C; (d) 65 °C.

The possibility of flow-induced chain orientation (and associated changes in intrinsic birefringence) may create concern about using flow birefringence to study the ODT in our solution under shear. However, the ODT measured under *all* flow conditions agrees with that measured in a *quiescent* sample for which flow-induced chain stretching is excluded (Figure 2a). Further, above the ODT there is *no* measurable flow-induced birefringence, even at the highest shear rates studied. This indicates that at these temperatures, any flow-induced chain stretching leads to an intrinsic birefringence which is negligible compared to the birefringence (form and intrinsic) associated with the microphase separated lamellar morphology.

3.3. Alignment in Oscillatory Shear Flow. Most studies of flow alignment in block copolymers have been performed using large amplitude oscillatory flow. In this section, we examine the flow alignment processes of our PS−PI solution over a range of frequencies and temperatures to establish the extent to which we observe behavior comparable to that previously documented in PS−PI melts.

Figure 4 presents a summary of rheo-optical flow alignment experiments carried out at a fixed strain of 200%, in which birefringence is measured in the 1−3 plane as a function of time during oscillatory shear flow. In all cases, the birefringence rapidly grows to a finite positive value of around 0.8×10^{-4}. Depending on the strain amplitude, the birefringence then either continues to increase more gradually, or begins to decrease toward zero. Generally speaking, higher frequencies favor a return to zero birefringence at long time; however, at the highest temperature studied, the birefringence remained large and positive over the entire frequency range accessible in the optical flow cell.

During the alignment process, the measured intensity transmitted between crossed polarizers ($I^{\perp}$) only exhibited small fluctuations over an oscillation cycle. The 1−3 projection of the refractive index tensor is evidentally not very sensitive either to periodic rocking of the lamellar normals within individual cycles or to any shear induced chain stretching (a potential concern at high frequencies). Instead, this observation supports the notion that, even during the shearing, these birefringence measurements provide a reliable indicator of the development of macroscopic alignment in the lamellar orientation state.

The results in this figure are generally consistent with those of Gupta and co-workers[18,19] and Patel and co-workers.[14] Positive birefringence values in this geometry are indicative of perpendicular character in the orientation state. It appears that at low frequencies, the solution tends toward perpendicular alignment, although at the lowest temperature the alignment develops very gradually. At higher frequencies, it has been previously reported that large amplitude oscillatory shear results in parallel alignment.[12,14,18,19] Zero birefringence in the 1−3 plane is consistent with this assessment, which may be more directly tested using oblique light paths (see below). It thus appears that our solution exhibits a transition from perpendicular to parallel alignment with increasing frequency, consistent with observations in melts. Other experiments on our solution have confirmed that it is possible to change from perpendicular to parallel alignment at fixed frequency by increasing the strain amplitude,[36] again in line with previous results in melts.[20] In the high-frequency regime, Gupta and co-workers reported that the path by which parallel alignment is achieved may also depend on frequency.[18,19] At the frequencies studied here, we always observe a positive transient $\Delta n_{1,3}$, which means that the transient state is relatively depleted of transverse orientation, giving it perpendicular character. Since we are limited by the frequency

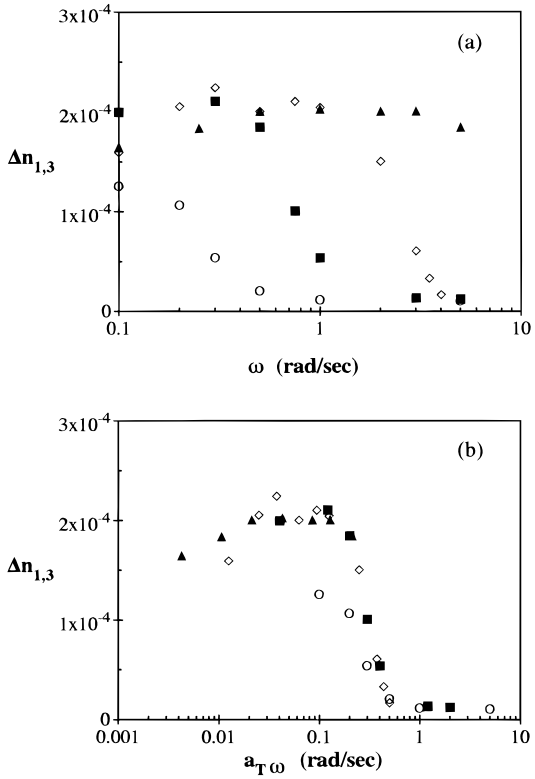

Figure 5. Birefringence measured after 10,000 seconds of large amplitude oscillatory shear at a constant strain of 200%: (a) unshifted data, (b) data shifted using shift factors calculated by eq 7. T = 25 °C (○), 35 °C (■), 50 °C (◇), 65 °C (▲).

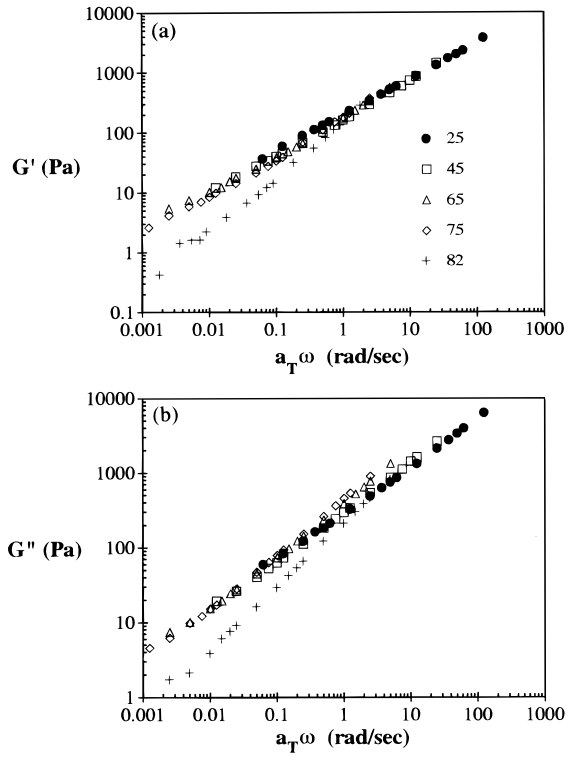

Figure 6. (a) Storage and (b) loss moduli measured on an ordered but random sample. Frequency axes were shifted using eq 7.

that can be applied in our optical flow cells, we do not know whether our solution might show a negative birefringence transient at higher frequency such as that reported by Gupta and co-workers,[18,19] reflecting an initial depletion of perpendicular layers.

To further characterize the effect of temperature on flow alignment dynamics, Figure 5 presents birefringence measured after 10 000 s of oscillatory shear as a function of frequency for the four temperatures studied. Although it is clear that this does not provide enough time to reach steady conditions at the lower temperatures, this does provide a convenient basis to classify the alignment character. This plot shows the transition from perpendicular to parallel alignment dynamics with increasing frequency and demonstrates that the transition frequency increases as the temperature is raised. To reduce these frequency dependent results at different temperatures, we use time−temperature shifting, with shift factors determined from rheological data on our solution.

Figure 6 presents the linear dynamic properties measured for a range of temperatures below the ODT, and one temperature above the ODT. Below the ODT, both G' and G'' show power law behavior, with a much weaker frequency dependence than that expected for flexible polymers in the terminal regime ($G' \sim \omega^2$, $G'' \sim \omega$). The observed near power law dependence is typical of the dynamic behavior observed in ordered PS−PI melts. It is seen that time−temperature shifting allows the data to be roughly superimposed, using shift factors given by:

$$a_T = (6.14 \times 10^{-12})e^{7672/T(\mathrm{K})} \qquad (7)$$

Dynamic data obtained above the ODT, not surprisingly, cannot be superimposed on data for the ordered solution. However, as discussed previously, they also do not show the expected terminal scalings for disordered flexible polymers, perhaps due to sensitivity limitations on the transducer at these high temperatures where relaxation is quite rapid. At the same time, we do find that the data obtained in the disordered state do agree with the ordered data for frequencies above 1 rad/s (at T_{ref} = 25 °C). It is thus reasonable to assume that the relative enhancement in moduli below this frequency occurs as a result of the viscoelasticity of the layered structure, while above this frequency, molecular-level dynamics dominate.

Returning to the rheo-optical data, Figure 5b shows that the shift factors obtained rheologically allow effective reduction of the flow alignment dynamics, consistent with the observations of Patel and co-workers.[14] Specifically, we find that the reduced frequency of the transition from perpendicular to parallel alignment, ∼0.3−0.4 rad/s, is comparable to the frequency range where rheological data suggest the regimes of layer and molecular viscoelasticity are separated. At the lowest reduced frequencies, the results still show significant positive birefringence, with no sign of a transition back to a parallel orientation state as observed by Zhang et al.[25] This is not surprising, however, since we adopt a thermal history (heating above the ODT, and then cooling to the test temperature) that does not include the extended annealing believed to be necessary to yield this low frequency parallel regime.[27]

As noted earlier, zero measured birefringence in the 1−3 plane is consistent with parallel alignment, but confirms neither it nor provides a measure of the quality of the orientation state. Using the oblique light path methods described in section 2.3.3, it is possible to characterize the degree of alignment achieved by oscil-

Table 1. Measurements of Birefringence following Oscillatory Shear Alignment in Parallel Prism Flow Cell

$T = 25$ °C, $\omega = 1$ rad/s, $\gamma_o = 150\%$, $t = 5000$ s

θ, deg	$\Delta n(\theta)$	Δ
30	$-5.0\ (\pm 0.6) \times 10^{-5}$	$-2.0\ (\pm 0.25) \times 10^{-4}$
60	$-1.4\ (\pm 0.2) \times 10^{-4}$	$-1.9\ (\pm 0.25) \times 10^{-4}$

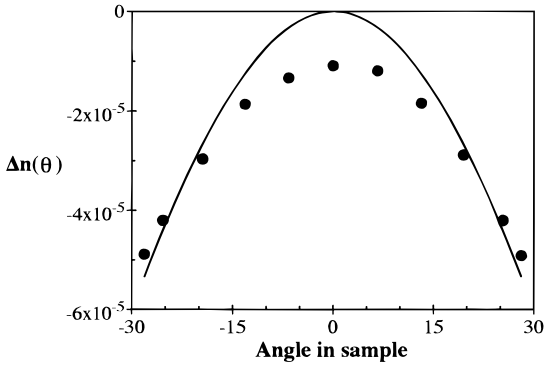

Figure 7. Birefringence vs angle of light path through the sample, measured in rotating disk flow cell. Sample was previously flow aligned under conditions identical to those used in Table 1. Solid curve represents predictions of eq 4, using $\Delta = -2 \times 10^{-4}$.

latory flow at high frequencies. The specialized flow cells for these measurements are, however, limited to room-temperature experiments.

In oscillatory shear flow, the parallel prism device described by Brown et al. is expected to provide the best measure of in-plane orientation, since it allows light to pass through the sample at comparatively steep angles.[41] It turned out to be impossible to monitor the evolution of orientation from an isotropic initial condition in this flow cell, since either loading a sample at room temperature or cooling the entire flow cell from above the ODT resulted in squeeze flow that imparted a significant degree of parallel orientation in the initial quiescent sample. However, application of prolonged oscillatory shear flow at 150% strain and a frequency of 1 rad/s further enhanced the orientation and led to a reproducible final state irrespective of the initial condition of the sample.

Table 1 summarizes measurements of birefringence made in this flow cell at the two oblique angles, based on several runs using two different sample thicknesses. Assuming the uniaxial symmetry expected for parallel alignment, eq 4 may be used to extract the underlying optical anisotropy, Δ, from the measured values of $\Delta n(\theta)$. As seen in Table 1, measurements at both 30 and 60° lead to values of $\Delta \approx -2 \times 10^{-4}$. Self-consistency between the values obtained at the two separate angles supports the hyphothesis that the orientation state is indeed uniaxial.

The full rotating disk flow cell used by Hongladarom and Burghardt[40] for oblique light path measurements could be heated above the ODT and cooled to room temperature without inducing significant orientation in the solution. With this flow cell, then, it was possible to shear the fluid under conditions equivalent to those used in Table 1 to verify that the final state was independent of the initial condition. Figure 7 presents measurements of birefringence as a function of light path angle within the sample (having accounted for refraction effects). This flow cell does not allow for as steep light paths as the parallel prism device, but except for deviations observed at small angles due to baseline offset (see section 2.3.4), results obtained in this flow cell are consistent with those in Table 1. (These results provide a useful benchmark of the manifestations of a well-defined parallel orientation state in the rotating disk flow cell for comparison with later results obtained in steady shear, since the parallel prism device cannot be used in that case.)

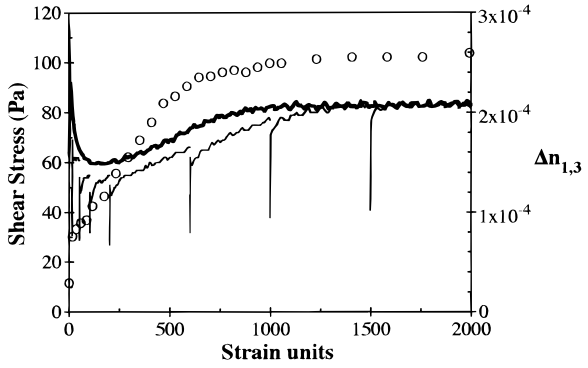

Figure 8. Steady shear flow alignment experiments conducted at 25 °C and a shear rate of 0.292 s^{-1}. Starting from a random orientation state, shear stress was measured as a function of time during continuous shearing (heavy line) or during intermittent shearing (light lines). Birefringence measurements from a separate flow alignment experiment are represented by circles.

The birefringence value obtained by high frequency oscillatory shear is remarkably (probably fortuitously) close to the estimate of form birefringence given in section 2.3.1. Examination of Figure 5 shows that it is also roughly equal in magnitude to the largest *positive* birefringence observed in the low-frequency regime, in which perpendicular alignment is expected. It thus seems that a birefringence of -2×10^{-4} is likely to be near the value of the monodomain value (Δn_o) for this solution and that oscillatory shear flow is capable of inducing high degrees of both parallel and perpendicular alignment. At room temperature, Figure 4a shows that oscillatory shear imparts perpendicular orientation very slowly, so that at this temperature, perpendicular alignment at low-frequency never attains perfection comparable to that achieved in parallel alignment at high frequency. This was further demonstrated using oblique light methods during low-frequency oscillatory flow alignment at room temperature, where despite prolonged shearing, the expected signature of $\Delta n(\theta) =$ constant (eq 5) was never achieved.[36] These room temperature, low-frequency results are contrasted by the low-frequency behavior at higher temperatures, Figure 4b−d, where significant perpendicular alignment ($\Delta n_{1,3} = 2 \times 10^{-4}$) is readily obtained.

3.4. Alignment in Steady Shear Flow. Results in the preceding section indicate that our PS−PI solution shows flow alignment phenomena in oscillatory shear consistent with previous observations in PS−PI melts. We now turn to a discussion of steady shear flow, for which much less systematic data have been gathered. We start with a detailed discussion of results obtained at room temperature, since in this case measurements are available both in the 1,3 plane and using oblique light path methods to assess the orientation state resulting from applied shear.

3.4.1. Alignment Studies at Room Temperature. Figure 8 presents results of mechanical and rheo-optical flow alignment experiments conducted at room temper-

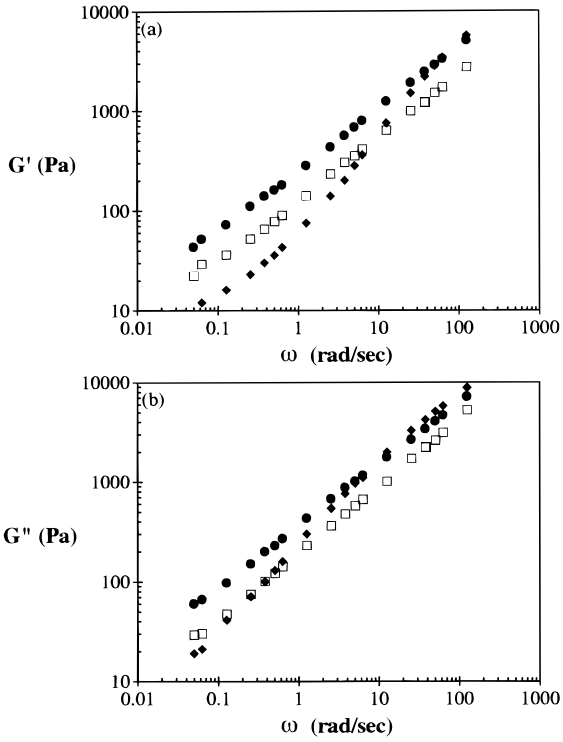

Figure 9. (a) Storage and (b) loss modulus vs frequency, during intermittent steady shear flow alignment at 0.292 s^{-1} and 25 °C: (●) initial, unaligned sample; (□) following 200 strain units; (◆) sample following 4000 strain units.

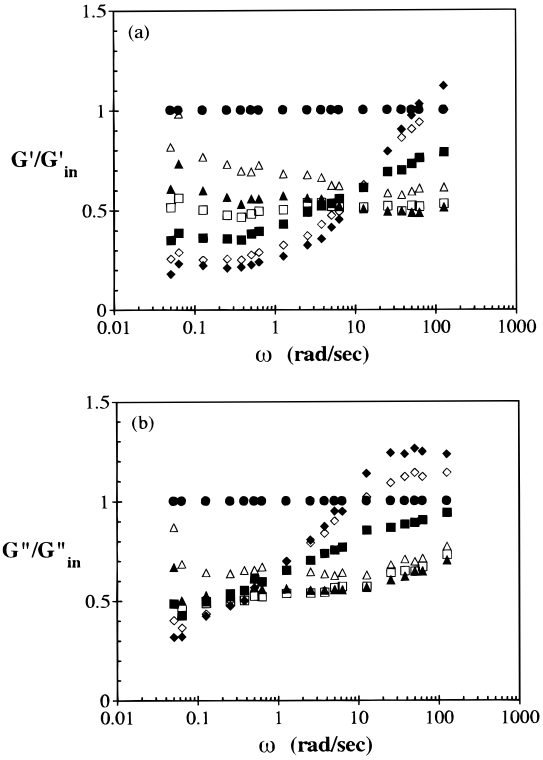

Figure 10. (a) Storage and (b) loss modulus vs frequency, normalized by initial values, during intermittent steady shear flow alignment at 0.292 s^{-1} and 25 °C. Frequency sweeps performed after (△) 15, (▲) 50, (□) 200, (■) 600, (◇) 1000, and (◆) 4000 strain units.

ature, using the same steady shear flow rate. In both cases, the sample is heated above the ODT to erase thermal and flow history and then cooled to room temperature prior to initiating shear flow. The heavy curve in Figure 8 shows measurements of shear stress as a function of applied strain during the flow alignment. Roughly 1000 strain units are required to reach steady state conditions. Initially, the shear stress drops rapidly, up to applied strains of near 150 units. Then, the stress begins to grow again, more slowly increasing to around 35% above its minimum value. The symbols in this figure represent results of an analogous rheo-optical experiment, in which birefringence in the 1,3 plane is monitored as a function of applied strain. These data also show signs of a fast process, in which birefringence initially increases to around 8×10^{-5}, and a slower process, in which $\Delta n_{1,3}$ continues to grow, ultimately achieving a large, positive value. These fast and slow processes correspond closely to the initial drop and subsequent growth in shear stress measured mechanically.

Further mechanical characterization of the evolution of fluid structure during steady shear flow alignment was obtained by intermittent flow experiments where shear was periodically stopped to perform linear viscoelasticity experiments. As seen in Figure 8, measurements of shear stress as a function of total accumulated strain using this intermittent shear flow protocol yield similar results to those obtained in continuous shear. In particular, the initial drop and subsequent increase in shear stress are both repeated. Although there are differences in detail, these results suggest that fluid structure is only slightly affected by the intermittent delays during the flow alignment.

Figure 9 presents storage and loss modulus vs frequency for (i) an initially unaligned sample, (ii) a sample after shearing for a total of 200 strain units (near the stress minimum in Figure 8), and (iii) a sample after 4000 strain units (steady-state conditions). The initial portion of the flow alignment leads to a uniform drop of around 50% in both storage and loss moduli. Further shear leads to deeper reduction in the low-frequency moduli, while at high-frequency both storage and loss moduli *increase*, ultimately to values higher than the initial state for an unaligned polydomain sample.

These results are similar to data of Gupta and coworkers,[19] obtained in oscillatory flow alignment of PS−PI melts under low-frequency oscillatory flow alignment leading to perpendicular orientation. An initial fast process led to a certain level of positive $\Delta n_{1,3}$, accompanied by a uniform drop in G' and G''. Subsequent shearing then led to a high degree of perpendicular alignment, accompanied by strong enhancements in the high-frequency moduli.[19] Figure 10 presents more complete data on the evolution of moduli in our solution, normalized by their initial values for the unoriented sample. We see that the initial drop in modulus occurs very rapidly (like the initial drop in shear stress), while the subsequent growth in high-frequency modulus occurs more slowly. In the final steady-state conditions, enhancements are observed in G'' at roughly an order of magnitude lower frequencies than the enhancements in G'.

When Figure 10 is compared with Figure 8, it seems clear that the drop and growth of shear stress measured during the flow alignment and the evolution in moduli reflect the same underlying changes in fluid structure. In particular, the slow development of large positive values of $\Delta n_{1,3}$, indicative of a high degree of perpendicular alignment, is accompanied by a mechanical signature of enhanced high-frequency moduli. In low-

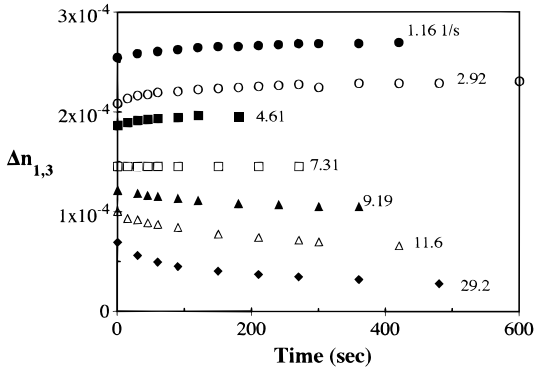

Figure 11. Changes in birefringence observed upon cessation of flow at the indicated shear rate. For shear rates <10 s^{-1}, 1500 strain units were applied; for shear rates >10 s^{-1}, 300 strain units were applied.

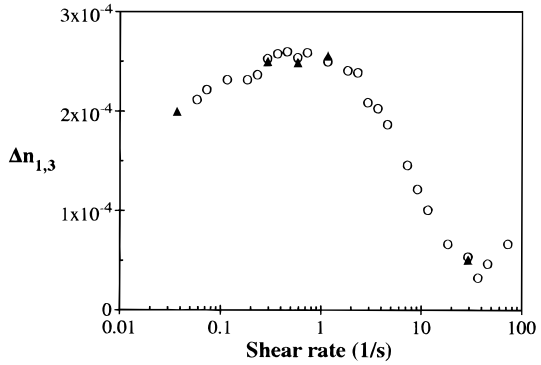

Figure 12. Birefringence measured immediately after shearing at 25 °C for 1500 strain units (rates <10 s^{-1}) or 300 strain units (rates >10 s^{-1}). Circles represent an experiment in which shear rate was incrementally increased. Triangles represent experiments in which the sample was subjected to shear from a random state.

frequency oscillatory flow alignment, Gupta and coworkers attribute the initial fast growth of $\Delta n_{1,3}$ (and drop in moduli) to a depletion of transverse orientation, while the subsequent slow growth of birefringence represents a transformation of the system to a high degree of perpendicular character.[19] In a perpendicularly aligned lamellar structure, both blocks must bear the full applied strain, so that if either block has a high modulus this will necessarily translate into a large modulus for the sample as a whole. A growth in moduli accompanying development of perpendicular orientation can thus indicate the sort of viscoelastic contrast that is believed to influence flow alignment dynamics.[14] Although our PS−PI solution is far from its glass transition, considerable viscoelastic contrast is evidently present. Indeed, the extent of enhancement in the high-frequency moduli observed in Figure 10 is greater than that observed by Gupta et al. in a PS−PI melt.[18] Apart from this difference in detail, it appears that development of perpendicular alignment in steady shear at low rates is very similar to perpendicular alignment at low frequencies in oscillatory shear.

The phenomena illustrated in Figures 8−10 are typical of steady shear flow alignment experiments at rates below around 1 s^{-1}. As shear rate is increased, the behavior changes significantly. One example is provided by Figure 11, which shows measurements of birefringence as a function of time following cessation of shear flow. Below 1 s^{-1}, there is very little change in fluid structure upon cessation of flow, as inferred from the intermittent flow experiments discussed earlier, reflected by no observable changes in measured birefringence. In the range between 1 and 10 s^{-1}, a transition in behavior is observed in which the final birefringence decreases dramatically. In this regime also, there can be significant evolution in the value of the birefringence during the period following flow. Between 1 and 7 s^{-1}, the birefringence decreases with shear rate, but the sample relaxes toward more positive $\Delta n_{1,3}$ (that is, toward perpendicular orientation). Above 7 s^{-1}, the birefringence continues to decrease with applied shear rate, but during relaxation the sample relaxes toward zero $\Delta n_{1,3}$ (potentially ambiguous, but as will be shown below, toward parallel alignment). While these changes in birefringence upon flow cessation could be due to relaxation of flow-induced chain stretching (and hence changes in the intrinsic contribution to the birefringence), the time scale over which the birefringence evolves seems much too long for molecular retraction. Instead, we attribute these birefringence changes to a slow evolution in the lamellar orientation state upon flow cessation.

At a comparable shear rate, the steady shear rheology of the fluid seems to change abruptly. In mechanical experiments using a Couette fixture, significant rod climbing is observed, limiting the possible duration of applied shear to around 300 strain units.[36] Similar effects occur in the rotating disk optical flow cell, where prolonged shearing at high rates leads to expulsion of the sample and entrainment of air bubbles. These observations suggest that shear at high rates is accompanied by normal stress-driven secondary flows, rendering careful experiments more difficult. It turns out, however, that 300 strain units is sufficient to induce considerable orientation (see below).

Figure 12 presents measurements of birefringence, immediately after cessation of shear flow, as a function of applied shear rate. Several features of this plot are noteworthy. At low shear rates, a high degree of perpendicular orientation is achieved. Indeed, comparison to Figure 4a shows that, at room temperature, steady shear flow is considerably more effective at promoting perpendicular alignment than oscillatory shear. The magnitude of the birefringence measured near 1 s^{-1} *exceeds* that measured using oblique light methods for parallel alignment induced by high frequency oscillatory shear (Table 1) and the estimate of form birefringence of our solution based on pure component refractive indices. Evidently, a very high degree of perfection in perpendicular alignment is possible. This is particularly interesting since previous steady-state measurements on PS−PI melts and solutions have generally yielded orientation states that, while possibly mixed, appear to be dominated by *parallel* alignment.[12,22] To our knowledge, this is the first report of predominantly perpendicular orientation induced by steady shear flow in a lamellar block copolymer.

The perpendicular character may also be assessed by using the oblique light methods in the rotating disk flow cell. Figure 13a presents measurements of birefringence as a function of the light path angle in the sample. Consistent with the predictions of eq 5, we observe that birefringence in this geometry is essentially independent of the angle at which light passes through the sample within the shear plane.

Returning to Figure 12, the transition between shear rates of 1 and 10 s^{-1} appears to be indicative of a transition between perpendicular and parallel align-

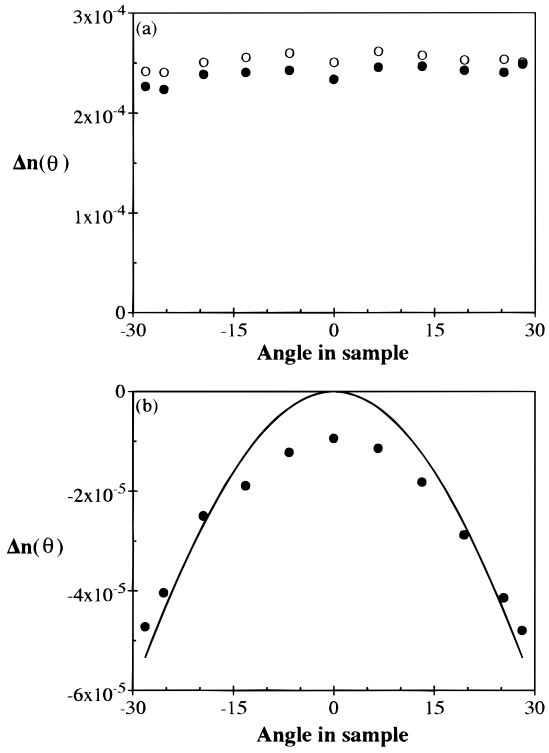

Figure 13. Birefringence as a function of angle of light path through quiescent sample, measured in rotating disk flow cell at 25 °C. (a) Measurements after 1500 strain units were applied to initially random samples, at rates of (●) 0.292, and (○) 1.16 s^{-1}. (b) Measurements after 300 strain units were applied at a rate of 29.2 s^{-1}. solid curve represents predictions of eq 4, using $\Delta = -2 \times 10^{-4}$.

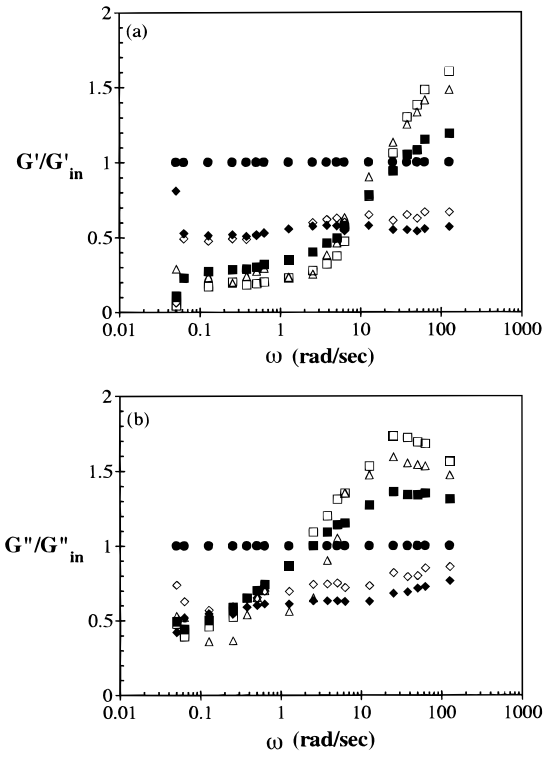

Figure 14. (a) Storage and (b) loss modulus vs frequency, normalized by values measured on unaligned sample, after shear flow alignment at (△) 0.292, (□) 1.16, (■) 4.61, (◇) 11.6, and (◆) 18.5 s^{-1}.

ment, analogous to the transition in flow alignment dynamics with increasing frequency in large amplitude oscillatory shear. Another possibility, however, is that steady shear at high rates simply disrupts the macroscopic alignment leading to low $\Delta n_{1,3}$. (Indeed, Wang et al. even suggest shear-induced *disordering* of a lamellar microphase separated structure in large amplitude oscillatory flow;[23] note, however, that their measurements were conducted much closer to the ODT than the present studies.) Here again, the oblique light path methods prove helpful. Figure 13b shows measurements of birefringence vs light path angle for a sample that had been sheared at 29.2 s^{-1} for 300 strain units. If measurements are attempted immediately after shear, the data are not very clean.[36] As seen in Figure 11, the magnitude of $\Delta n_{1,3}$ relaxes following cessation of shear flow, eventually reaching the limits of measurement due to the baseline difficulties alluded to earlier. The data in Figure 13b were obtained following this relaxation period and show indications of parallel alignment of comparable perfection to that obtained in high-frequency large amplitude oscillatory shear.

On the basis of these results, it seems clear that the transition in Figure 12 is indeed a flipping transition from perpendicular to parallel alignment. However, although steady flow at high rates tends to drive the system to parallel alignment, the orientation state generated during shear is imperfect, perhaps due to flow-induced defects in the parallel orientation state. (This may also be related to the possible presence of elastic-driven secondary flows at high shear rates). Following flow, the orientation distribution gradually relaxes to a more perfect parallel orientation state, with lower $\Delta n_{1,3}$ and the signature of parallel alignment expected in the oblique light path experiment, according to eq 4. Mechanical experiments show considerable evolution in the *low* frequency moduli during the 20 min following cessation of shear at 29.2 s^{-1},[36] again consistent with annealing of defects toward a more perfect parallel orientation.

Most of the data in Figure 12 were obtained by incrementally increasing the shear rate in discrete steps. As a result, although shear strain was limited to 300 strain units per point at high rates, the total accumulated strain could be quite large. Additional experiments were performed on samples with initially random alignment, obtained by thermal clearing and cooling to room temperature. In all cases, results were self-consistent with those obtained on the presheared sample. This is important in the case of the high shear rate data. By the time the incrementally stepped experiment reaches 29.2 s^{-1}, considerable total strain has been accumultated, but essentially identical results (including oblique light measurements) are obtained on a sample sheared from isotropic conditions for only 300 strain units at this rate. This demonstrates that these (comparatively) modest strains are sufficient to induce macroscopic alignment of high quality in the high shear rate limit.

Finally, Figure 14 presents linear viscoelastic measurements on samples that had been shear aligned in the rheometer using steady shear flow protocols similar to the optical experiments. For low shear rates that yield high final perpendicular alignment, the data exhibit the strong enhancement in high-frequency modulus identified earlier. The extent of the enhancement in modulus appears to be a reliable indicator of the extent of perpendicular character (i.e., $\Delta n_{1,3}$). Conversely, at high shear rates which lead to parallel

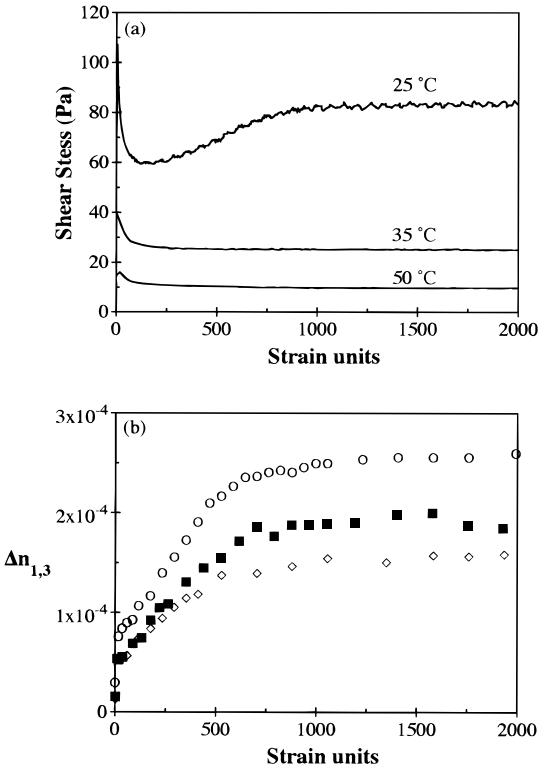

Figure 15. Effect of temperature on steady shear flow alignment at 0.292 s^{-1}, starting from macroscopically unaligned sample. (a) Shear stress vs shear strain. (b) Birefringence vs shear strain. Key: (○) 25 °C; (■) 35 °C; (◇) 50 °C.

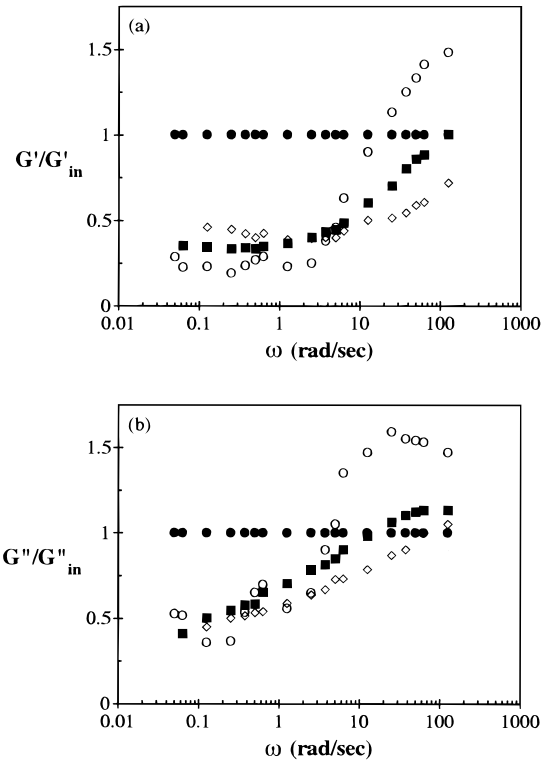

Figure 16. (a) Storage and (b) loss modulus vs angular frequency. Moduli are measured following application of 1500 strain units at 0.292 s^{-1}, and values are normalized by values measured on a macroscopically unaligned sample. Key: (○) 25 °C; (■) 35 °C; (◇) 50 °C.

alignment, the moduli merely show an essentially uniform drop in modulus, consistent with mechanical measurements of linear viscoelasticity on PS−PI melts that had been shear aligned to parallel alignment using high-frequency oscillatory flow.[14,19]

These results again provide direct indication of viscoelastic contrast, where perpendicularly aligned samples exhibit significant enhancements in high-frequency modulus relative to parallel samples. Patel and coworkers suggest that oscillatory flow alignment is driven by the tendency of the sample to adopt a configuration (parallel or perpendicular) in which the magnitude of the complex modulus is minimized.[14] Using data from Figure 14, the magnitude of $G^*(\omega)$ for a well-aligned perpendicular sample (1.16 s^{-1}) may be compared with that of a well-aligned parallel sample (18.5 s^{-1}). At high frequencies, the perpendicular sample has the greater G^*, while at low frequencies the parallel sample has the greater G^*. The crossover occurs at $\omega \approx 0.8$ rad/s, which is near the frequency at which oscillatory flow alignment switches modes (Figure 5) and at which the linear rheology of disordered and random ordered samples diverges (Figure 6). In all these respects, the behavior of our PS−PI solutions also seems quite consistent with that seen in PS−PI melt by Patel and co-workers.[14]

3.4.2. Effect of Temperature on Steady Flow Alignment. Figure 15 presents data for steady flow alignment experiments analogous to those of Figure 8 at higher temperatures. In all cases, the shear stress exhibits an initial, rapid drop upon inception of flow. However, at higher temperatures there is no subsequent increase in shear stress over long time scales such as that observed at room temperature. Figure 15b shows that this does not result from a lack of a slower process in the development of macroscopic alignment. Indeed, the growth of $\Delta n_{1,3}$ is very similar at all temperatures, including the large strains necessary to achieve steady state. The steady-state birefringence values do, however, decrease with increasing temperature. If the slower increase in stress is associated with development of perpendicular alignment, then a reduction in the ultimate perfection of the alignment may have an influence on the magnitude (or existence) of the resulting increase in shear stress.

Additional insight is provided by considering the dynamic moduli that result from steady shearing under the conditions of Figure 15. Figure 16 presents storage and loss moduli measured after the solution was sheared to steady state at each temperature, normalized by their initial values for a macroscopically unaligned sample. As seen before, development of perpendicular orientation leads to strong enhancements in dynamic moduli at high frequency. Results from Figures 8−10 suggest that this enhancement in modulus also plays a role in the long time scale growth of shear stress. In Figure 16, we see that as temperature is increased, the high-frequency moduli are enhanced, but to a lesser degree than at room temperature. This may reflect in part the different final degree of perpendicular alignment (Figure 15b), but also results from the fact that all dynamics are shifted to faster time scales as temperature increases. Thus, although shearing at a constant rate of 0.292 s^{-1} leads to similar growth of perpendicular orientation at these temperatures, the dynamic processes responsible for enhanced moduli (and growth of shear stress during steady shearing) are shifted to faster time scales and are likely not accessed at this relatively low shear rate. In fact, if both frequency and shear rate are shifted using eq 7, we obtain generally self-

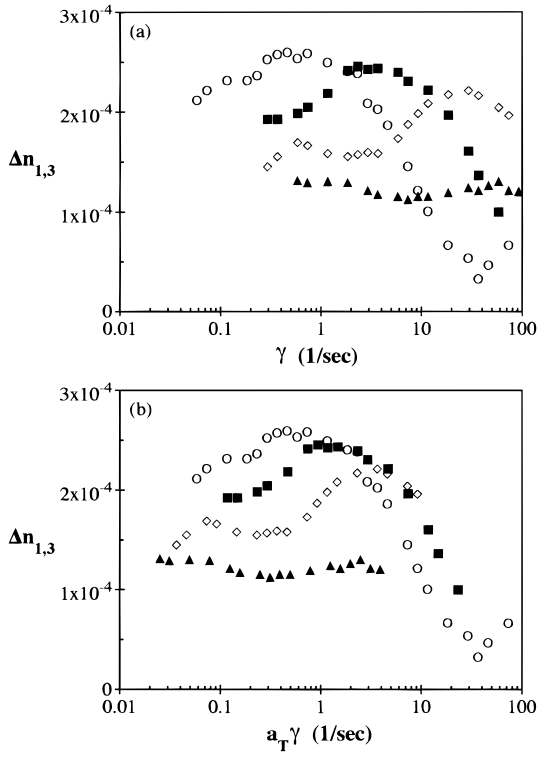

Figure 17. (a) Birefringence measured after shearing for 1500 strain units (low rates) or 300 strain units (high rates), plotted against applied shear rate: (○) 25 °C; (■) 35 °C; (◇) 50 °C; (▲) 65 °C. (b) Same data, plotted against shear rate shifted using eq 7 [T_{ref} = 25 °C].

consistent results concerning the linear viscoelastic properties resulting from flow alignment at low rates, regardless of temperature.[36]

Figure 17a presents measurements of birefringence as a function of steady shear rate for four different temperatures, collected using methods similar to those described in the previous section. At the two lowest temperatures, there are strong indications of a transition from perpendicular to parallel alignment with increasing shear rate; the transition shear rate is shifted upward with increasing temperature. At still higher temperatures, we can no longer access sufficiently high shear rates to verify that such a transition continues to be present. Figure 17b presents the same data, in which shear rate has now been shifted using eq 7. Time−temperature shifting is reasonably successful in reducing the data in the vicinity of the transition from parallel to perpendicular alignment. It is noteworthy that the flipping transition in steady shear occurs at significantly higher shear rates in steady shear than in oscillatory shear. This suggests that the location of flipping is determined by more than just shear rate magnitude. Away from the transition, the reduction of data is less successful than that in Figure 5b. In particular, in the low shear rate regime which clearly yields perpendicular alignment at low temperatures, the measured birefringence drops significantly with increasing temperature, also seen in Figure 15.

One possible explanation for lower birefringence at higher temperatures would be that, in fact, the perpendicular alignment remains of high quality but that the local anisotropy of the lamellar structure decreases due to increased mixing of styrene and isoprene segments as the ODT is approached. However, this is inconsistent with the oscillatory flow alignment results presented in Figure 5. At 65°, low frequency, large amplitude oscillatory flow induces highly oriented perpendicular alignment with a positive birefringence near 2×10^{-4}. Indeed, for temperatures of 35, 50, and 65 °C, the birefringence measured in oscillatory flow at low frequency depends very little on temperature. Conversely, at 65 °C steady shear flow leads to a birefringence of around 1.2×10^{-4}. Although steady shear flow is capable of producing stronger perpendicular alignment than oscillatory flow at room temperature, the opposite seems to be true as the temperatures approach the ODT.

As noted earlier, little work has been done studying flow alignment dynamics under steady shear flow in diblock PS−PI. Winey and co-workers report results from a few experiments in which a initially parallel PS−PI melt was subjected to steady shear flow. It was found that shear generated defect structures which could be visualized by TEM, while SAXS measurements revealed some spreading of a predominantly parallel orientation state in the gradient−vorticity plane.[12] These experiments were carried out quite far below the ODT, where oscillatory shear flow alignment yielded parallel orientation. Balsara et al. studied a PS−PI solution, similar to the present system, at a single shear rate and at a point quite close to the ODT.[22] They report an orientation state characterized as "rippled sheets that lie parallel to the shearing surface."[22] That is, the orientation state is again predominantly parallel, but with imperfections that in this case are sufficient to lead to easily measurable anisotropy in the flow−vorticity plane. Such a structure would show a positive birefringence in the geometry used in Figure 17.

At low temperatures, our steady birefringence results indicate two distinct regimes, in which perpendicular alignment is favored at low shear rates, and parallel alignment is favored at high shear rates. This is very similar to the dynamics exhibited in oscillatory shear flow, extensively studied in PS−PI melts and confirmed here for our solution. On this basis, one expects that in our experiments at higher temperatures, *both* oscillatory and steady shear flow should promote perpendicular orientation, since they lie in the low (reduced) frequency range. Figure 5 certainly bears this out for the case of oscillatory shear flow, but Figures 15 and 17 show poorer perpendicular alignment. Since these measurements are conducted closer to the ODT, the report by Balsara et al. of a mixed orientation state, with some perpendicular and some parallel character, may have bearing.[22] Although direct comparison is impossible since a characteristic material time cannot be identified from these results,[22] the development of complex, mixed orientation states under *steady* shear flow near the ODT could explain the differences found here between Figure 5 and Figure 17. In any event, these results show that, despite similarities in flow alignment dynamics well below the ODT, shear flow and oscillatory flow can have rather different effects on the alignment state of lamellar systems. Further steady shear flow experiments, ideally using scattering techniques to characterize the potentially complex orientation state, are necessary to explore these issues more deeply.

4. Conclusions

In oscillatory shear flow alignment, our results on a PS−PI solution are generally consistent with those reported in PS−PI melts. Parallel alignment is found

at high reduced frequencies, while perpendicular alignment results from low reduced frequencies. The critical frequency dividing these regimes is close to that where linear viscoelastic data above and below the ODT diverge from one another, as has been previously noted in melts.[14,18] In addition, near the critical frequency, increasing shear strain is able to effect a transition from perpendicular to parallel alignment,[36] again in agreement with observations in melts.[20] The presence of parallel alignment at high frequencies was confirmed and quantified using birefringence measurements with oblique light paths, thereby circumventing ambiguities associate with zero birefringence in the flow−vorticity plane. We did not observe a return to parallel alignment at low frequencies,[25] probably due to the thermal history applied to our samples prior to alignment experiments.[27]

In steady shear, we find that flow with low shear rates is capable of inducing a significant degree of perpendicular alignment, contrary to limited previous steady flow measurements on PS−PI block copolymers which indicated only defective parallel alignment.[12,22] Well below the ODT, the generation of perpendicular alignment with steady shear flow seems to occur in two steps. In a rapid initial step, birefringence increases to about one-third of its final value, while shear stress decreases dramatically and linear moduli drop nearly uniformly. In a slower second step, the birefringence increases to its final steady value, reflecting improving perpendicular alignment, accompanied by an increase in shear stress and increases in linear moduli at high frequencies. Many of these processes closely mimic the behavior during perpendicular alignment in PS−PI melts using large amplitude oscillatory flow at low frequency.[19] At these low temperatures, there is strong evidence of a transition from perpendicular to parallel alignment dynamics with increasing steady shear rate. Oblique light path birefringence measurements again provide assistance in classifying and quantifying both perpendicular and parallel alignment. There is a strong connection between the degree of perpendicular alignment and the presence of enhanced linear moduli at high frequency. Samples with parallel orientation show no enhancement in the high-frequency modulus. These observations are also similar to observations in PS−PI melts[14] and suggest that viscoelastic contrast plays a significant role in the high shear rate/high-frequency flow alignment dynamics, despite the fact that all measurements were conducted at least 100 °C above the depressed glass transition of the polystyrene block.

As temperature increases, the degree of perpendicular alignment obtained at low shear rates decreases. At the highest temperature studied, there is a significant difference in the quality of perpendicular alignment (as characterized by birefringence in the flow−vorticity plane) obtained by oscillatory flow alignment in comparison to steady flow alignment. Specifically, oscillatory flow gives a birefringence magnitude that is roughly 60% higher than that obtained in steady shear flow at 65 °C. It is possible that steady shear flow results in highly defective and/or mixed parallel/perpendicular orientation states as the temperature approaches the order−disorder transition. Thus, despite many similarities observed between steady and oscillatory shear flow, there are fundamental differences that warrant further attention.

Finally, no evidence was found for any shear flow-induced changes in the order−disorder transition temperature of our solution, using both large amplitude oscillatory or steady shear flow over a wide range of deformation rates.

Acknowledgment. This work was supported by the National Science Foundation through a Young Investigator Award, CTS-9457083, with matching funds from Procter and Gamble. We thank Professor John Torkelson for supplying the PS−PI block copolymer used in this work. Assistance with characterization was provided by Mike Myers and Tim Heitman at the Dow Chemical Company, and Matthew DeWitt at Northwestern University.

References and Notes

(1) Bates, F. S.; Fredrickson, G. H. *Annu. Rev. Phys. Chem.* **1990**, *41*, 525. Fredrickson, G. H.; Bates, F. S. *Annu. Rev. Mater. Sci.* **1996**, *26*, 501.
(2) Keller, A.; Pedemonte, E.; Willmouth, F. M. *Colloid Polym. Sci.* **1970**, *238*, 25.
(3) Folkes, M. J.; Keller, A.; Scalisi, F. P. *Colloid Polym. Sci.* **1973**, *251*, 1.
(4) Hadziioannou, G.; Mathis, A.; Skoulios, A. *Colloid Polymer. Sci.* **1979**, *257*, 136.
(5) Pakula, T.; Saijo, K.; Kawai, H.; Hashimoto, T. *Macromolecules* **1985**, *18*, 1294.
(6) Morrison, F. A.; Winter, H. H. *Macromolecules* **1989**, *22*, 3533.
(7) Morrison, F. A.; Winter, H. H.; Gronski, W.; Barnes, J. D. *Macromolecules* **1990**, *23*, 4200.
(8) Almdal, K.; Bates, F. S.; Mortensen, K. *J. Chem. Phys.* **1992**, *96*, 9122.
(9) Almdal, K.; Koppi, K. A.; Bates, F. S.; Mortensen, K. *Macromolecules* **1992**, *25*, 1743.
(10) Albalak, R. J.; Thomas, E. L. *J. Polym. Sci., Polym. Phys. Ed.* **1993**, *31*, 37.
(11) Koppi, K.; Tirrell, M.; Bates, F. S.; Almdal, K.; Colby, R. H. *J. Phys. II* **1992**, *2*, 1941.
(12) Winey, K. I.; Patel, S. S.; Larson, R. G.; Watanabe, H. *Macromolecules* **1993**, *26*, 2542.
(13) Winey, K. I.; Patel, S. S.; Larson, R. G.; Watanabe, H. *Macromolecules* **1993**, *26*, 4373.
(14) Patel, S. S.; Larson, R. G.; Winey, K. I.; Watanabe, H. *Macromolecules* **1995**, *28*, 4313.
(15) Pinheiro, B. S.; Hajduk, D. A.; Gruner, S. M.; Winey, K. I. *Macromolecules* **1996**, *29*, 1482.
(16) Polis, D. L.; Winey, K. I. *Macromolecules* **1996**, *29*, 8180.
(17) Kannan, R. M.; Kornfield, J. A. *Macromolecules* **1994**, *27*, 1177.
(18) Gupta, V. K.; Krishnamoorti, R.; Kornfield, J. A.; Smith, S. D. *Macromolecules* **1995**, *28*, 4464.
(19) Gupta, V. K.; Krishnamoorti, R.; Chen, Z.-R.; Kornfield, J. A.; Smith, S. D.; Satkowski, M. M.; Grothous, J. T. *Macromolecules* **1996**, *29*, 875.
(20) Gupta, V. K.; Krishnamoorti, R.; Kornfield, J. A.; Smith, S. D. *Macromolecules* **1996**, *29*, 1359.
(21) Balsara, N. P.; Hammouda, B. *Phys. Rev. Lett.* **1994**, *72*, 360.
(22) Balsara, N. P.; Hammouda, B.; Kesani, P. K.; Jonnalagadda, S. V.; Straty, G. C. *Macromolecules* **1994**, *27*, 2566.
(23) Wang, H.; Kesani, P. K.; Balsara, N. P.; Hammouda, B. *Macromolecules* **1997**, *30*, 982.
(24) Okamoto, S.; Saijo, K.; Hashimoto, T. *Macromolecules* **1994**, *27*, 5547.
(25) Zhang, Y.; Wiesner, U.; Spiess, H. W. *Macromolecules* **1995**, *28*, 778.
(26) Zhang, Y.; Wiesner, U. *J. Chem. Phys.* **1995**, *103*, 4784.
(27) Zhang, Y.; Wiesner, U.; Yang, Y.; Pakula, T.; Spiess, H. W. *Macromolecules* **1996**, *29*, 5427.
(28) Zhang, Y.; Wiesner, U. *J. Chem. Phys.* **1997**, *106*, 2961.
(29) Maring, D.; Wiesner, U. *Macromolecules* **1997**, *30*, 660.
(30) Major, M. D. An Examination of the Organization of Block Copolymer Containing Systems by Fluorescence Spectroscopy. Ph.D. Dissertation, Northwestern University, 1989.
(31) Brandrup J.; Immergut, E. H. *Polymer Handbook*, 3rd ed.; Wiley: New York, 1989.
(32) Prud'homme, J.; Roovers, J. E. L.; Bywater, S. *Euro. Polym. J.* **1972**, *8*, 901.

(33) Balsara, N. P.; Perahia, D.; Safinya, C. R.; Tirrell, M.; Lodge, T. P. *Macromolecules* **1992**, *25*, 3896.
(34) Frederickson, G. H.; Leibler, L. *Macromolecules* **1989**, *22*, 1238.
(35) Lodge, T. P.; Pan, C.; Jin, X.; Liu, Z.; Zhao, J.; Maurer, W. W.; Bates, F. S. *J. Polym. Sci., Polym. Phys. Ed.* **1995**, *33*, 2289.
(36) Zryd, J. L. Dyanmics of Alignment Processes in a Lamellar Polystyrene-Polyisoprene (PS−PI) Diblock Copolymer Solution under Shear Flow. Ph.D. Dissertation, Northwestern University, 1996.
(37) Lodge, T. P.; Fredrickson, G. H. *Macromolecules* **1992**, *25*, 5643.
(38) Born, M.; Wolf, E. *Principles of Optics;* Pergamon Press: New York, 1959; pp 702−705.
(39) Hongladarom, K.; Ugaz, V. M.; Cinader, D. K.; Burghardt, W. R.; Quintana, J. P.; Hsiao, B. S.; Dadmun, M. D.; Hamilton, W. A.; Butler, P. D. *Macromolecules* **1996**, *29*, 5346.
(40) Hongladarom, K.; Burghardt, W. R. *Macromolecules* **1994**, *27*, 483.
(41) Brown, E. F.; Burghardt, W. R.; Kahvand, H.; Venerus, D. C. *Rheol. Acta* **1995**, *34*, 221.
(42) Brown, E. F.; Burghardt, W. R. *J. Rheol.* **1996**, *40*, 37.
(43) Balsara, N. P.; Garetz, B. A.; Dai, H. J. *Macromolecules* **1992**, *25*, 6072.
(44) Olvera de la Cruz, M. *J. Chem. Phys.* **1989**, *90*, 1995.
(45) Cates, M. E.; Milner, S. T. *Phys. Rev. Lett.* **1989**, *62*, 1856.
(46) Koppi, K.; Tirrell, M.; Bates, F. S. *Phys. Rev. Lett.* **1993**, *70*, 1449.
(47) Runyon, J. R.; Barnes, D. E.; Rudd, J. F.; Tung, L. H. *J. Appl. Polym. Sci.* **1969**, *13*, 2359.
(48) Tung, J. H. *J. Appl. Polym. Sci.* **1979**, *24*, 953.

MA971091W